Correct and efficient initiation of viral RNA synthesis by the influenza A virus RNA polymerase

Judith Oymans[1±], Aartjan J.W. te Velthuis[1,2*]

[1]Sir William Dunn School of Pathology, University of Oxford, South Parks Road, OX1 3RE, Oxford, United Kingdom. [2]Clarendon Laboratory, Department of Physics, University of Oxford, Parks Road, OX1 3PU, United Kingdom.

*Corresponding author e-mail: aartjan.tevelthuis@path.ox.ac.uk

[±]Present address: Wageningen Bioveterinary Research, Houtribweg 39, 8221 RA Lelystad, The Netherlands

Short title: Influenza virus RNA synthesis
Figures: 5
Words main text: 4727

Keywords: Influenza virus, RNA-dependent RNA polymerase, replication, transcription, priming loop, realignment

Abstract

The influenza A virus uses an RNA-dependent RNA polymerase (RdRp) to replicate and transcribe its genome. To ensure that the genome is copied correctly, the RdRp has been proposed to realign the initiation product of viral RNA (vRNA) synthesis from the internal initiation site to the 3' end of the complementary RNA (cRNA) template before extending the nascent vRNA. Here we show that this process is essential for viral RNA synthesis and that the RdRp uses a mechanism involving the priming loop to enforce realignment during replication. We also find that realignment plays a role in viral mRNA synthesis, enabling the RdRp to handle sequence variation among the primers that it snatches from host mRNAs to prime viral mRNA synthesis. Overall, these observations advance our mechanistic understanding of how the influenza A virus initiates replication and transcription correctly and efficiently.

Introduction

Negative strand RNA viruses infect a wide variety of birds and mammals, and they use an RNA-dependent RNA polymerase (RdRp) to copy and transcribe their viral RNA genome. One of the best-studied examples of this type of RdRp is the influenza A virus (IAV) RdRp[1,2]. The IAV genome consists of eight segments of single-stranded, negative sense viral RNA (vRNA) that are each bound by one copy of the viral RdRp and multiple copies of the viral nucleoprotein (NP)[1,2]. Together, vRNA, RdRp and NP form a viral ribonucleoprotein complex (vRNP) that is imported into the nucleus of the host cell. Here the vRNP replicates the vRNA via a complementary RNA (cRNA) intermediate and transcribes the vRNA to form viral mRNAs[1,2]. The latter molecules are exported from the nucleus and translated by cellular ribosomes, while cRNAs are bound by new NP and RdRp molecules, forming cRNPs capable of synthesising vRNAs[3].

The IAV RdRp consists of the viral proteins polymerase basic protein 1 (PB1), polymerase basic protein 2 (PB2), and polymerase acidic protein (PA)[1,4]. The PB1 subunit, the N-terminal third of PB2 and the C-terminal two-thirds of PA form the conserved core of the polymerase domain[5-7]. This central core contains four channels, including a template entry and exit channel, a nucleotide entry tunnel, and a product RNA exit channel[8,9]. The remaining parts of PA and PB2 form flexible domains at the periphery of the polymerase domain, which are important for binding and cleaving cellular host mRNAs, a process that yields capped RNA primers for viral transcription[1,4].

The viral RdRp binds the 5' and 3' terminal ends of the vRNA or cRNA, also called the vRNA or cRNA promoter respectively[10-12], via a surface-binding pocket above the NTP channel[5,6,13]. The 3' end of either promoter can transiently translocate to the active site[14], allowing *de novo* initiation on terminal 3' UC of the vRNA (Fig. 1a) or *de novo* initiation at positions 4U and 5C of the 3' terminus of the cRNA (Fig. 1a)[15,16]. The two initiation mechanisms are markedly different. First, terminal *de novo* initiation on a vRNA promoter, but not internal *de novo* initiation on a cRNA promoter, critically depends on the PB1 priming loop to stabilise the initiating ATP (Fig. 1a)[15]. Second, internal initiation requires realignment of the pppApG initiation

product to bases 3' 1U and 2C of the cRNA prior to elongation[15,16] (Fig. 1a). A failure to perform this realignment step would generate a vRNA lacking 3 nucleotides at its 5' terminus. Since the vRNA 5' terminus is part of the vRNA promoter and critical for the activity and conformational changes of the influenza virus RdRp[5-7], such a truncated vRNA would likely not support efficient cRNA and mRNA synthesis. It is believed that a number of negative strand RNA viruses use a realignment process to ensure faithful replication of their genome[16-18], but the molecular mechanism by which these viruses control realignment is unknown.

In addition to cRNA synthesis, the IAV virus RdRp can use the vRNA promoter to initiate viral transcription. By contrast to replication, viral mRNA synthesis requires a capped RNA primer of 8-14 nucleotides[19,20], which the RdRp snatches from nascent host RNA polymerase II (Pol II) transcripts after binding to the Pol II C-terminal domain[21,22]. When these capped primers are hybridised to the 3' terminus of the vRNA template (Fig. 1a), they are extended from position 2 or 3 of the vRNA template, depending on the sequence of the primer[19,23-25], and polyadenylated on a poly(U)-tract 16 nucleotides downstream of the 5' terminus of the vRNA[26]. There is presently no mechanistic explanation for how the IAV may initiate transcription with primers that have no sequence complementarity to the 3' terminus of the vRNA template[27,28].

In this study we use a combination of structure-guided mutagenesis, *in vitro* polymerase activity assays, and cell-based RNP reconstitution assays to show that realignment during vRNA synthesis is essential for IAV replication and that the IAV RdRp uses its priming loop to enforce prime-realignment during vRNA synthesis. In addition, we demonstrate how a mechanistically different type of realignment occurs during transcription initiation as a function of the primer sequence and the interaction of the primer with the priming loop. Our observations provide a mechanistic insight into IAV RNA synthesis and redefine the function of the priming loop as the platform controlling faithful and efficient replication and transcription initiation.

Results

Prime-realignment is essential for viral RNA synthesis

A side-by-side comparison of the activity of the IAV RdRp on a vRNA or cRNA promoter shows that ApG extension is ~30% weaker on the cRNA promoter (Fig. 1b). A similar observation was recently made for activities of the influenza B virus RdRp on the influenza B virus vRNA and cRNA promoters[9]. This difference in promoter activity may be explained, at least in part, by the realignment step that is required for the extension of the nascent vRNA after internal initiation on the cRNA promoter (Fig. 1a). To study how the IAV RdRp coordinates this realignment step, we attempted to measure the formation of failed realignment (FR) products in ApG extension assays using influenza A/WSN/33 virus RdRp preparations. Crucially, ApG extension after realignment requires UTP incorporation, while a failed realignment event utilises ATP for extension (Fig. 1a). To favour the latter event, we either doubled the ATP concentration or omitted UTP from the reaction. Under the latter conditions, we observed a loss of the 15 nt full-length (FL) product and the appearance of a 12 nt major product (Fig. 1c). This 12 nt product was not synthesised in reactions where 4U of the 3' cRNA strand mutated to A (4U→A) to prevent internal elongation. This suggests that FR products can be detected and identified *in vitro*, but that they are usually not synthesised by the wild-type RdRp.

To investigate whether the prime-realignment mechanism was controlled upstream and/or downstream of the active site, we either replaced the first G-C base pair of the duplex of the cRNA promoter with an A-U base pair to make it less stable (Supplemental Fig. 1) or engineered alanine substitutions of PB1 residues S269, L271, P272 or V273 (S269A, L271A, P272A and V273A, respectively), which are part of a conserved helix-turn-helix that guides the A-form helix of template-product duplex away from the active site (Supplemental Fig. 2a and b). A PB1 mutant containing alanine substitutions of two critical active site aspartates (PB1 DD445-446AA; PB1a)[29] served as negative control. No increase in FR product formation was observed in reactions containing the mutant cRNA promoter duplex or PB1 mutants S269A and L271A. By contrast, mutant P272A failed to extend the ApG dinucleotide (Fig. 1d), while mutant V273A produced significantly more FR products than wild-type (Fig. 1d). Mutation V273A had no effect on

heterotrimer formation, *de novo* initiation, ApG extension on a vRNA promoter, or transcription initiation (Supplemental Fig. 2c-g), suggesting that this mutation affects realignment specifically. To confirm that the V273A FR product had been produced through internal elongation, we measured the activity of V273A on the 4U→A mutant promoter and observed a reduction in the FR signal without impairment of FL production (Fig. 1e). Mutation of 1U of the cRNA 3' strand to A (1U→A), which prevents realignment, left FR formation unaffected but greatly impaired FL product formation for all RdRps tested (Fig. 1f).

To investigate the activity of V273 in cell culture, we used a mini replicon assay that relies on the reconstitution of vRNPs from plasmid-expressed IAV RdRp subunits, NP and a segment 6 (neuraminidase (NA)-encoding) vRNA template. The synthesis of the viral RNA species (vRNA, cRNA and mRNA) was measured using primer extensions with reverse transcriptase (RT) and 5' radiolabelled primers (Supplemental Table 1). As shown in Fig. 1f, viral RNA synthesis by V273A, but also S269A, was impaired and showed a differential effect on cRNA and mRNA synthesis (Fig. 1g). These observations corroborate previous RNP reconstitutions[30] and experiments showing that mutations V273A, V273L or V273D reduce the fitness of A/WSN/33 viruses by >90%[31]. Taken together, the above suggest that an increase in failed realignment events affects viral replication and transcription.

The priming loop modulates prime-realignment during vRNA synthesis

The priming loop of the IAV RdRp resides downstream of the active site (Fig. 2a). Research of other RNA virus RdRps has shown that priming loops plays a role in the selection against double-stranded RNA (dsRNA) and the correct positioning of the single-stranded RNA (ssRNA) template in the active site[32-34]. Analysis of PB1 priming loop mutant Δ648-651 previously showed that elongation increases during both replication and transcription after the deletion of the tip of the priming loop[15], suggesting that the priming loop limits the transition from initiation to elongation. To investigate if FR product formation was affected by the priming loop, we engineered seven deletions in the influenza A/WSN/33 (H1N1) virus PB1 subunit based on the different

conformations of the priming loop in current crystal structures (Fig. 2b) and the sequence conservation of the priming loop among influenza A, B and C viruses (Fig. 2c). In RNP reconstitutions, all mutants (Fig. 2c) were significantly impaired in viral RNA synthesis (Fig. 2d). This result was expected for mutants Δ648-651, Δ642-656 and Δ631-662, which all lack the tip residues that are critical for the initiation of cRNA synthesis[15]. The impaired activity of the mutants Δ656-662, Δ631-642, Δ636-642 and Δ631-635 suggests that also the middle and N- and C-terminal anchor points of the priming loop play an important role in RdRp activity.

The RNP reconstitution assay described above confirmed that the PB1 priming loop is important for viral RNA synthesis, but it did not allow us to observe effects on RNA polymerase assembly, or transcription and replication-specific affects due to the interdependence of these activities in cell culture (e.g., some amplification of the template vRNA is required to observe mRNA signals above background). To study these aspects in more detail, the wild-type RdRp, the PB1a mutant, and our seven deletion mutants were expressed in 293T cells and purified by IgG chromatography. SDS-PAGE analysis of the purified proteins showed that all nine recombinant enzymes were able to form heterotrimers, with the three subunits present at and equal ratio (Supplemental Fig. 3a). This suggests that our deletions in the priming loop had not affected RdRp assembly.

Next, we performed ApG extension assays on a cRNA promoter. We observed that mutants Δ648-651 and Δ642-656 exhibited a higher activity compared to the wild-type enzyme and a significantly higher production of the FR product (Fig. 2e). In the case of mutant Δ636-642, the total activity was composed of an increase in FR product synthesis and a reduction in FL product formation. FL product synthesis was also significantly impaired in reaction containing mutant Δ642-656, but increased in reactions containing mutant Δ648-651 (Fig. 2e), in line with our previous observations[15]. The activity of the remaining three priming loop mutants was greatly impaired (Fig. 2e). To verify that the observed FR product was synthesised due to a failure in the realignment mechanism, we replaced the wild-type cRNA promoter with the 1U→A promoter to prevent realignment (Fig. 2f) or the 4U→A promoter to

prevent internal elongation (Fig. 2g). We found that mutants Δ648-651, Δ642-656, and Δ636-642 were still able to produce the failed realignment product on the 1U→A promoter (Fig. 2f), but not on the 4U→A promoter (Fig. 2g).

To investigate whether the effect of the priming loop on ApG extension was promoter-specific, we analysed the activity of the mutants in the presence of the vRNA promoter. Mutants Δ648-651 and Δ642-656 exhibited a higher activity compared to the wild-type enzyme, while the activity of the Δ636-642 mutant was indistinguishable from wild-type (Fig. 2h). In all three reactions, no differential change in the pattern was observed (Fig. 2h), suggesting that realignment during replication happens on the cRNA promoter only. The four remaining priming loop mutants showed greatly impaired activities compared to wild-type (Fig. 2h). Overall, these results are consistent with a model in which the priming loop stimulates realignment during IAV vRNA synthesis and suppresses internal extension. The effect on vRNA promoter activity may be linked to a conformational change that is required to allow the nascent strand to leave the RdRp[15], as observed for other RdRps[35].

The reduced activity of mutants Δ631-662, Δ656-662, Δ631-642 and Δ631-635 can be caused by impaired promoter binding or a structural change in the RdRp. To measure RdRp-promoter complex formation, we used a single-molecule Förster resonance energy transfer (sm-FRET)-based binding assay[15,36]. The FRET distribution of the fluorescently labelled RNA in solution resulted in an apparent FRET population with a mean and standard deviation of E^*=0.76±0.09 (Supplemental Fig. 3b). Addition of the wild-type RdRp resulted in a shift to a lower apparent FRET due to a change in the RNA structure upon binding, while incubation with a promoter-binding mutant (Tetra mutant)[15] resulted in no shift in the apparent FRET population (Supplemental Fig. 3b). When we incubated the fluorescently labelled RNA with mutant Δ632-662 we observed a shift in the FRET population similar to the wild-type RdRp (Supplemental Fig. 3b), demonstrating that promoter binding is not affected by a complete deletion of the PB1 priming loop. We next incubated the priming loop mutants with a capped, 20-nt long RNA to test cap cleavage and the conformational change that the influenza RdRp

undergoes upon promoter binding[1,7]. We observed that the activities of Δ631-662, Δ656-662, Δ631-642 and Δ631-635 were greatly impaired (Supplemental Fig. 3c). By contrast, the activity of mutants Δ648-651, Δ642-656 and Δ636-642 was indistinguishable from wild-type (Supplemental Fig. 3b), suggesting that these mutants were folded and binding the viral promoter correctly, while the other four mutants had an unknown structural impairment.

Realignment during transcription is guided by 3' U1 and U4 of the vRNA template

IAV transcription does not initiate *de novo*, but uses a capped RNA primer that is hybridised to 3' 1U and/or 2C of the vRNA promoter and then extended from 3' 2C or 3G (Fig. 3a). It is currently assumed that this process is largely dependent on Watson-Crick base pairing, although transcription initiation without base pairing has been observed[19,24,25,27,28]. Interestingly, it was recently reported that IAV mRNAs isolated from infected cells contain 4-nucleotide repeats downstream of the capped primer[19,25,28]. These repeats correspond to the first 4 nucleotides of the 3' end of the vRNA and may be introduced by the IAV RdRp using a prime-realign mechanism[19,25,28].

To investigate whether the realigment process during transcription was mechanistically similar to the prime-realign mechanism of vRNA synthesis, we incubated a 20-nt radiolabelled capped RNA primer with IAV RdRp purified from insect cells and followed its cleavage and subsequent extension in time (Fig. 3b). Cleavage of the provided radiolabelled RNA results in a capped 11 nt long RNA with a 3' terminal AG that is complementary to the 3' UC of the vRNA (Fig. 3b). As shown in Fig. 3b, cleavage and extension of the radiolabelled RNA resulted in one major product initiated likely from 3G (i.e., the G-product or GP) and several slower migrating minor products. This pattern is identical to that observed in assays relying on β-globin mRNA as primer donor[37-41]. To investigate the initiation site, we mutated the 3' 2C of the vRNA promoter to A (2C→A) and observed a loss of the GP signal and a concomitant increase in the signal that migrated 1 nt slower, suggesting that it had likely initiated from 2C (i.e., the C-product or CP). To exclude that the CP signal had been synthesised following an alternative cleavage event (i.e., with

a primer having a different 3' terminal base), we incubated the IAV polymerase with a radiolabelled capped 11-mer containing 3' AG. This reaction resulted in one major product and at least two slower migrating bands (Fig. 3c). Introduction of the 2C→A mutant promoter resulted in a loss of the fast migrating GP signal and an increase in 1 nt slower CP signal (Fig. 3c). In a further control reaction, in which we used a primer ending in 3' CA, only the CP signal was observed (Supplemental Fig. 4a). Together, these results establish the identity of the GP and CP signals and they suggest that a primer with a 3' terminal AG can either initiate at 3' 3G after base pairing with the 3' UC of the vRNA or at 3' 2C after non Watson-Crick base pairing with the 3' U (Fig. 3b). By contrast, a primer ending in 3' A will likely initiate from 3' 2C after base pairing with 3' U, consistent with previous reports[19,24,25].

All transcription reactions contain at least one additional minor, slow migrating product that is synthesised at a slower rate than the GP and CP signals and longer than the template (Fig. 3d, Supplemental Fig. 4b). To investigate whether this was a realignment product (RP) synthesised, we mutated 1U to A (1U→A) or 4U to A (4U→A) in the 3' strand of the vRNA promoter. Mutation 1U→A resulted in a loss of both the CP signal and the additional minor product, while mutation 4U→A resulted in a loss of the minor RP signal only (Fig. 3e). A similar result was obtained when we mutated 4U to C (4U→C) (Supplemental Fig. 4c), a sequence variant that down-regulates transcription of segments 1, 2 and 3 of the IAV genome[42]. These findings provide direct evidence that the IAV RdRp can catalyse a realignment event during transcription initiation[19,25] and that 3' terminal residues 1U and 4U of the vRNA promoter guide this process (Supplemental Fig. 4d).

Primer length and duplex stability determine realignment probability

To investigate the role of base pairing during transcription and realignment in more detail, we replaced the terminal G of the AG primer with U (i.e. creating a 3' AU primer). On the wild-type vRNA promoter, this AU primer was efficiently extended, forming a major CP signal and minor GP and RP bands. On the 1U→A mutant promoter the realignment product was not present, while the GP and CP signals were unaffected (Fig. 4a), suggesting that

Watson-Crick base pairing at position 1 of the vRNA does not improve initiation. However, on the 2C→A mutant promoter, which supports A-U Watson-Crick base pairing, the CP signal was reduced as expected and, to our surprise, realignment upregulated and equal to the GP signal (Fig. 4a). The increase in realignment appears inversely correlated with the drop in the base pair stability between the wild-type template and 3' AG primer promoter-primer duplex ($\frac{AGCA}{UCGU}$, Fig. 3c) and the 2C→A template and the 3' AU primer promoter-primer duplex ($\frac{AUCA}{UAGU}$, Fig. 4a). This suggests that the realignment probability is partly dependent on the stability of promoter-primer base pairing.

The above observation does not explain why the wild-type template and 3' AU primer promoter-primer duplex ($\frac{UGCA}{UCGU}$, Fig. 4a) produces similar realignment levels as the 3' AG primer that is extended on the wild-type promoter (Fig. 3c). To investigate this, we performed a transcription reaction in the presence of a capped RNA primer that ended in 3' UG. Although this primer is extended into a $\frac{UGCA}{UCGU}$ promoter-primer duplex on the wild-type template, similar to the 3' AU primer on the wild-type vRNA promoter, its extension leads to the formation of equal levels of GP and RP signals (Fig. 4b). The 3' AU and 3' UG primers have in common that only 9 bases of the capped 11-mer remain single-stranded after transcription initiation on 3G, while 10 bases remain single-stranded when the RdRp uses AU to initiate on 3' 2C. Altogether, these results suggest that realignment during transcription is affected by two factors: i) Watson-Crick base pairing between the template and the primer, and ii) the ssRNA length of the primer. Interestingly, the latter implies that some component of the RdRp interacts with the primer to suppress realignment.

The priming loop suppresses realignment during transcription

The priming loop is situated between the active site and the entrance of the nascent strand exit channel and ideally positioned to interact with the incoming capped primer (Fig. 2a, Supplemental Fig. 5). To test whether the priming loop affects realignment during IAV transcription, we incubated the

priming loop truncation mutants (Fig. 2c) with a radiolabelled capped 11-mer ending in 3' AG and NTPs. Measurement of the synthesised CP and GP signals showed that mutants Δ648-651 and Δ642-656 extended a capped primer more efficiently than the wild-type enzyme (Fig. 4c). This suggests that in the wild-type enzyme, the tip and β-sheet of the priming loop limit elongation of the capped RNA primer, in line with previous observations[15]. By contrast, mutant Δ636-642 synthesised CP and GP levels that were indistinguishable from wild-type, while the four other priming loop mutants showed impaired primer extension levels (Fig. 4c), likely as a result of the deletions in the N- and C-terminal anchors of the priming loop.

Measurement of the RP signal showed that transcriptional realignment was increased in reactions containing mutants Δ648-651, Δ642-656 and Δ636-642 (Fig. 4c). After correction for the differences in the transcriptional activity by normalising the RP signal to the sum of the CP and GP levels (CP+GP), we found that the realignment efficiency of Δ648-651 was indistinguishable from wild-type, while mutants Δ642-656 and Δ636-642 showed significantly increased realignment efficiencies compared to wild-type. These results imply that the β-strand of the priming loop suppresses prime-realignment during transcription, in contrast to the prime-realignment mechanism that the RdRp uses for vRNA synthesis (Fig. 2). Due to the absence of sequence conservation in the β-strand of the loop (Fig. 2c), future crystallographic studies will be required to identify the interaction mechanism.

Discussion

The PA endonuclease of the IAV RdRp preferentially cleaves mRNAs 3' of G moieties, generating primers ending in 3' BG (where B is any base but A)[43,44]. However, other cleavage sites are possible[43,44]. A recent crystal structure of the influenza B virus RdRp bound to a vRNA template and capped primer showed that the 3' terminus of the vRNA can enter and even ‘overshoot’ the active site by 1 nt without duplex unwinding[9]. This places 2C and 3G in positions -1 and +1 of the active site (Fig. 5), ideal for transcription initiation with primers ending in 3' BG. In total, 6 nt of the 3' vRNA terminus are located in the template entry channel in this conformation (Fig. 5), while three (3' 7U, 8C and 9G) remain single-stranded between the duplex at the surface of

RdRp and the template entry channel[9]. Residues 7U and 8C are stacked in a T-orientation by residues of the PB2 subunit (the 'T-pocket'). It is likely that the interaction between PB2 and 7U is sequence specific as a 7U→A mutation was previously shown to abrogate *de novo* initiation[16]. Although no structure is available of the RdRp bound to the complete cRNA promoter, it is plausible that G9 will occupy the T-pocket when the cRNA 3' end enter the template channel (Fig. 5). Indeed, previous mutational data have shown that like 7U in the vRNA, G9 in the cRNA is essential for *de novo* initiation [16]. To support transcription initiation from 2C with primers ending in 3' A or U (Supplemental Fig. 4a and Fig. 4), residues 1U and 2C of the vRNA 3' terminus must be placed in positions -1 and +1 of the active site, respectively (Fig. 5). This can only occur if the 3' terminus of the vRNA backtracks 1 nt, leaving 5 nt in template entry channel. Although it is presently unknown where the additional unpaired base would go, it is likely that this is a frequent event given that we always observe significant initiation from 2C (Supplemental Fig. 4) even when initiation from 3G would be more stable.

Our analysis of transcription initiation confirms that the 4-nt duplications found in the 5' termini of IAV mRNAs[19,28] are the result of realignment of the extended capped primer from residue 4U to 1U of the vRNA 3' end. We also find that this mechanism is largely suppressed in the wild-type IAV RdRp, likely through interactions of the priming loop with the single-stranded part of the capped primer (Fig. 4). Presently, we do not understand the importance of the realignment mechanism in IAV RNA synthesis, but speculate that it may be a safeguard that can turn each cap-snatching event into a successful transcription initiation event. Interestingly, segments with a 3' 4C in the vRNA promoter instead of the canonical 3' 4U show little realignment (Supplemental Fig. 4c), which may explain why transcription is down regulated on these IAV genome segments[42]. This should be addressed in more detail in future studies.

There has been significant disparity in the literature about whether base pairing is essential for transcription initiation[19,23-25,27,28,43]. We find that base pairing between the primer and the template influences both transcription initiation and realignment, with 3' BG primers showing increased realignment

due to a reduced interaction with the priming loop and the template (Fig. 4 and Fig. 5). Primers ending in 3' A and U initiated preferentially from the 3' U of the wild-type vRNA promoter (Supplemental Fig. 4a and Fig. 4), although we can not exclude that downstream sequences may affect base pairing due to e.g. stacking energies. We also show that an interaction between the priming loop and the ssRNA part of the primer is important for limiting realignment. We propose that this is an additional measure that helps the IAV RdRp initiate efficiently after a cap-snatching event.

To support *de novo* initiation on the cRNA promoter, 8 nt must enter the template entry channel (Fig. 1a and Fig. 5). Our data show that reducing the stability of the cRNA promoter duplex does not increase initiation on a cRNA promoter (Supplemental Fig. 1), suggesting that 4U and C5 of the cRNA 3' promoter strand can be placed at positions -1 and +1 of the active site without duplex unwinding. The IAV RdRp may readily achieve this, because the cRNA 3' promoter strand is one nt longer than the vRNA 3' strand. After internal *de novo* initiation, the IAV RdRp realigns the initiation product to the 3' terminus of the cRNA[16] (Fig. 1a), which requires melting of the dinucleotide-template duplex and backtracking of the cRNA 3' terminus to allow the dinucleotide to rebind at U1 and C2 in positions -1 and +1 of the active site (Fig. 5). We have previously seen that the 3' end of the cRNA promoter can move freely in and out of the template channel in single-molecule experiments[14] and our observations here suggest that the priming loop and palm subdomain residue V273 may enforce this process by acting as elongation block (Fig. 2e and Fig. 5). Importantly, the priming loop does not induce realignment after terminal initiation on a vRNA promoter (Fig. 2). It is tempting to speculate that the stability of the vRNA template-tetramer duplex is sufficient to prevent melting and induce a conformational change in the priming loop (Fig. 5). Both ideas are consistent with observations from other RNA virus RdRps in which the priming loop must undergo a conformational change to allow the product duplex to egress the active site[35,45].

In the absence of a structure of the influenza virus RdRp elongation complex, we can only speculate about the mechanism through which V273 affects realignment. In both the apo structure of the influenza C virus RdRp[7]

and the influenza B virus RdRp bound to the cRNA 5' terminus[13], the PB2 cap binding domain closes the nascent strand exit channel via interactions with the helix-turn-helix of the palm subdomain and the PB2 mid-domain[1,7]. The PB2 cap binding domain will thus need to undergo a conformational change to allow the nascent strand to exit the polymerase. A recent study showed that deletion of the cap binding domain affects vRNA synthesis, but not cRNA synthesis[46]. It is possible that V273 may be involved in the packing of the PB2 cap binding domain against the template exit channel and thus indirectly affecting elongation and realignment. Future studies will address this in more detail.

In summary, we have analysed how the IAV RdRp controls realignment during viral replication, a process that is a critical step in influenza virus RNA synthesis. We also find that the previously proposed realignment step during transcription is mechanistically different from realignment during vRNA synthesis and propose that it is suppressed by the priming loop when the capped primer stably base pairs with the template. Our findings offer new insights into influenza virus replication and transcription, and they may have implications for the many other RNA viruses that also rely on a prime-realign mechanism to replicate and/or transcribe their genome[18,47-49].

Material and methods

Cells and plasmids

Human embryonic kidney (HEK) 293T cells were originally sourced from the ATCC, mycoplasma tested and maintained in DMEM (Sigma) supplemented with 10% fetal calf serum (FCS). Plasmids pPolI-NA, pcDNA-NP, pcDNA-PB1, pcDNA-PA, pcDNA-PB2-TAP, and pcDNA-PB1a have been described previously[37,38,50]. Also the promoter binding mutant (PB1 R238A, R672A and PA K572A and K583A)[15], the priming loop mutant PB1 Δ648-651[15], the PA endonuclease mutant D108A[51], and the PB1 palm subdomain mutants S269A and V273A have been reported before[30]. To construct plasmids expressing additional mutant forms of the PB1 subunit, the plasmid pcDNA-PB1 was altered using side-directed mutagenesis with the primers (Life Technologies) listed in Supplemental

Table 2.

Sequence alignment and structural modelling

Amino acid sequences of the PB1 subunits of IAV A/WSN/33 (H1N1), influenza B virus B/Michigan/22687/09, and influenza C virus C/JJ/50 were aligned using ClustalX[52] and visualised using ESPript[53]. To model the poliovirus $3D^{pol}$ elongation complex (PDB 3OL7) into the influenza B virus RdRp crystal structure (PDB 5MSG), we aligned active site residues 324-332 of the poliovirus enzyme with residues 442-449 of the bat influenza virus PB1 subunit in Pymol 1.3. The influenza B virus PB1 subunit and the influenza C virus PB1 subunit (PDB 5D98) were aligned by active site residues 442-449.

Purification of recombinant influenza virus RNA polymerase

Wild type and mutant recombinant RdRp preparations were purified using tap affinity purification (TAP) tags on the C-terminus of the PB2 subunit[38]. The recombinant polymerases were expressed via transfection of 3 µg of PB1 or mutant PB1, PB2-TAP, and PA into HEK 293T cells using Lipofectamine^{2000} (Invitrogen). After 48 h the cells were lysed and the protein purified using IgG Sepharose (GE Healthcare) chromatography and cleavage by tobacco etch virus (TEV) protease (Invitrogen) in cleavage buffer (20 mM Hepes pH 7.5, 150 mM NaCl, 0.1% NP40, 10% glycerol, 1x PMSF and 1 mM DTT). The recombinant RdRp preparations were analysed by 8% SDS-PAGE and silver staining using a SilverXpress kit (Invitrogen). The concentration of the proteins was estimated in gel using a BSA standard. For activity assay, the RdRp preparations were stored in cleavage buffer at -80 ^{o}C. RdRp preparations for smFRET experiments were concentrated in 50 mM Hepes (pH 7.5), 10% glycerol, 500 mM NaCl, 0.05% *n*-Octyl β-D-thioglucopyranoside (OTG), and 0.5 mM tris(2-carboxyethyl)phosphine (TCEP) before storage at -80 ^{o}C. Recombinant RdRp preparations from insect cells were expressed as described previously[54].

RNP reconstitution assay

RNP reconstitutions were performed by transfecting plasmids expressing PB1 or mutant PB1, PA, PB2, and NP together with pPolI-NA into HEK 293T cells using Lipofectamine^{2000} (Invitrogen). Total RNA was isolated using Tri Reagent (Sigma) 24 h after transfection and analysed using primer extension assays as described previously[15]. Briefly, viral RNA species and a 5S rRNA loading control were reverse transcribed using ^{32}P-labelled primers (Supplemental Table 1) and SuperScript III (Invitrogen). cDNA synthesis was stopped with 10 µl loading buffer (90% formamide, 10% ddH_2O, 10 µM EDTA, xylene cyanole, bromophenol blue) and analysed by 6% denaturing PAGE (6% 19:1 acrylamide/bis-acrylamide, 1x TBE buffer, 7 M urea). The viral RNA species and the 5S rRNA signal were visualised using a FLA-500 scanner (Fuji) and analysed using AIDA (RayTek).

***In vitro* ApG extension assay**

ApG assays were performed as described previously[15]. To test the ApG extension activity, 4-µl reactions were performed that contained: 500 µM ApG (Jena Bioscience), 1 mM DTT, 500 µM UTP (unless indicated otherwise), 500 µM CTP, 500 µM ATP (unless indicated otherwise), 0.7 µM vRNA or cRNA promoter (Sigma), 5 mM $MgCl_2$, 1 U µl^{-1} RNAsin (Promega), 0.05 µM [α-^{32}P]GTP (3000 Ci mmole^{-1}, Perking-Elmer), 5% glycerol, 0.05% NP-40, 75 mM NaCl, 10 mM HEPES pH 7.5, and ~2 ng RdRp µl^{-1}. The reactions were incubated for 1 h at 30 °C and stopped with 4 µl loading buffer. The RNA products were analysed by 20% denaturing PAGE and visualised by phosphorimaging. P-values were determined using an unpaired non-parametric t-test.

Capping and labelling RNA primers

Synthetic 5' tri- or diphosphate-containing RNAs of 11 nt (Supplemental Table 3, Chemgenes) and 20 nt (Supplemental Table 3, Chemgenes) were capped with a radiolabelled cap-1 structure using 0.25 µM [α-

^{32}P]GTP (3,000 Ci mmole^{-1}, Perkin-Elmer), 2.5 U/µl 2'-O-methyltransferase (NEB) and a vaccinia virus capping kit (NEB) according the manufacturer's instructions. The products were analysed by 20% denaturing PAGE, excised from the gel and desalted using NAP-10 columns (GE Healthcare) equilibrated with RNase free water.

***In vitro* capped oligo cleavage assay**

To test the endonuclease activity of the IAV RdRp, we performed 3-µl reactions that contained: 1 mM DTT, 0.7 µM vRNA promotor (Sigma), 5 mM $MgCl_2$, 1 U µl^{-1} RNAsin (Promega), 1500 cpm capped 20-nucleotide long RNA primer, 5% glycerol, 0.05% NP-40, 75 mM NaCl, 10 mM HEPES pH 7.5, and ~2 ng RdRp µl^{-1}. The reactions were incubated for 1 hour at 30 °C, stopped with 4 µl loading buffer and analysed by 20% denaturing PAGE. The capped RNA cleavage products were visualised by phosphorimaging.

***In vitro* capped oligo nucleotide extension assay**

Capped RNA oligo extensions were performed as 4-µl reactions containing: 1 mM DTT, 500 µM UTP, 500 µM ATP, 500 µM CTP, 500 µM GTP, 5 mM $MgCl_2$, 1U/µl RNAsin (Promega), 1500 cpm capped RNA primer, 0.7 µM vRNA promotor (Sigma), 5% glycerol, 0.05% NP-40, 75 mM NaCl, 10 mM HEPES pH 7.5, and ~2 ng RdRp µl^{-1}. The reactions were incubated for 1 h at 30 °C, unless indicated otherwise, stopped with 4 µl loading buffer and analysed by 20% denaturing PAGE. The extended capped primers were visualised by phosphorimaging. P-values were determined using an unpaired non-parametric t-test.

***In vitro* dinucleotide synthesis assay**

The pppApG synthesis activity was measured as described previously[15]. Briefly, 3-µl reactions were set up that contained: 1 mM DTT, 350 µM adenosine, 5 mM $MgCl_2$, 1U µl^{-1} RNAsin, 0.05 µM [α-^{32}P] GTP (3000

Ci/mmole, Perking-Elmer), 0.7 μM vRNA or cRNA promotor (Sigma), 5% glycerol, 0.05% NP-40, 75 mM NaCl, 10 mM HEPES pH 7.5, and ~2 ng RdRp μl^{-1}. The reactions were incubated for 18 h at 30°C, inactivated for 2 min at 95 °C and then treated with 1 U calf intestine alkaline phosphatase (Promega) at 37°C for 30 min. The reactions were stopped with 4-μl loading buffer and analysed by 20% denaturing PAGE.

Single-molecule Förster resonance energy transfer

Promoter binding was measured as described previously[14,15,36]. Briefly, a Cy3 donor dye was placed on U17 of the 3' promoter strand and an Atto647N acceptor dye was placed on U6 of the 5' strand. The RNA oligonucleotides were synthesized by IBA, and labelled, purified, and annealed as described previously[36]. The excitation of the donor and acceptor fluorophores was measured using a custom-built confocal microscope with alternating-laser excitation (ALEX)[55,56]. In a typical experiment, ~100 nM RdRp was pre-incubated with 1 nM double-labelled promoter RNA in binding buffer (50 mM Tris-HCl (pH 8.0), 5% glycerol, 500 mM NaCl, 10 mM $MgCl_2$, 100 μg/ml BSA) for 15 min at 28 ^{o}C. Samples were diluted 10-fold in binding buffer before the measurements were performed at excitation intensities of 250 μW at 532 nm and 60 μW at 635 nm. The E^* values were plotted as one-dimensional distributions and fitted with a single Gaussian to obtain the mean E^* and the standard deviation.

Acknowledgements

The authors thank Dr Ervin Fodor, Dr. Nicole Robb, Dr. Achilles Kapanidis and Benjamin Nilsson for support and discussions. This work was funded by Wellcome Trust grant 098721/Z/12/Z (to AJWtV), grant 825.11.029 from the Netherlands Organization for Scientific Research (to AJWtV) and an Erasmus+ mobility grant (to JO).

Author contributions

AJWtV and JO performed experiments and analysed data. AJWtV wrote manuscript.

Competing interests

The authors have no competing interests.

References

1. te Velthuis, A. J. & Fodor, E. Influenza virus RNA polymerase: insights into the mechanisms of viral RNA synthesis. *Nat Rev Microbiol* **18,** 473-493 (2016).
2. Fodor, E. The RNA polymerase of influenza a virus: mechanisms of viral transcription and replication. *Acta Virol* **57,** 113-122 (2013).
3. York, A., Hengrung, N., Vreede, F. T., Huiskonen, J. T. & Fodor, E. Isolation and characterization of the positive-sense replicative intermediate of a negative-strand RNA virus. *Proc Natl Acad Sci U S A* **110,** E4238-E4245 (2013).
4. Pflug, A., Lukarska, M., Resa-Infante, P., Reich, S. & Cusack, S. Structural insights into RNA synthesis by the influenza virus transcription-replication machine. *Virus Research* **S0168-1702,** 30782-30781 (2017).
5. Reich, S., Guilligay, D., Pflug, A., Malet, H., *et al.* Structural insight into cap-snatching and RNA synthesis by influenza polymerase. *Nature* **516,** 361-366 (2014).
6. Pflug, A., Guilligay, D., Reich, S. & Cusack, S. Structure of influenza A polymerase bound to the viral RNA promoter. *Nature* **516,** 355-360 (2014).
7. Hengrung, N., El Omari, K., Serna Martin, I., Vreede, F. T., *et al.* Crystal structure of the RNA-dependent RNA polymerase from influenza C virus. *Nature* **527,** 114-117 (2015).
8. Gerlach, P., Malet, H., Cusack, S. & Reguera, J. Structural Insights into Bunyavirus Replication and Its Regulation by the vRNA Promoter. *Cell* **161,** 1267-1279 (2015).
9. Reich, S., Guilligay, D. & Cusack, S. An in vitro fluorescence based study of initiation of RNA synthesis by influenza B polymerase. *Nucleic acids research* **45,** 3353-3368 (2017).

10. Parvin, J. D., Palese, P., Honda, A., Ishihama, A. & Krystal, M. Promoter analysis of influenza virus RNA polymerase. *Journal of virology* **63,** 5142-5152 (1989).
11. Pritlove, D. C., Fodor, E., Seong, B. L. & Brownlee, G. G. In vitro transcription and polymerase binding studies of the termini of influenza A virus cRNA: evidence for a cRNA panhandle. *J Gen Virol* **76 (Pt 9),** 2205-2213 (1995).
12. Fodor, E., Pritlove, D. C. & Brownlee, G. G. The influenza virus panhandle is involved in the initiation of transcription. *J Virol* **68,** 4092-4096 (1994).
13. Thierry, E., Guilligay, D., Kosinski, J., Bock, T., *et al.* Influenza Polymerase Can Adopt an Alternative Configuration Involving a Radical Repacking of PB2 Domains. *Molecular Cell* **61,** 1-13 (2016).
14. Robb, N. C., te Velthuis, A. J., Wieneke, R., Tampé, R., *et al.* Single-molecule FRET reveals the pre-initiation and initiation conformations of influenza virus promoter RNA. *Nucleic Acids Res* **44,** 10304-10315 (2016).
15. te Velthuis, A., Robb, N. C., Kapanidis, A. F. & Fodor, F. The role of the priming loop in influenza A virus RNA synthesis. *Nature Microbiology* **1,** 16029 (2016).
16. Deng, T., Vreede, F. T. & Brownlee, G. G. Different de novo initiation strategies are used by influenza virus RNA polymerase on its cRNA and viral RNA promoters during viral RNA replication. *J Virol* **80,** 2337-2348 (2006).
17. Martin, A., Hoefs, N., Tadewaldt, J., Staeheli, P. & Schneider, U. Genomic RNAs of Borna disease virus are elongated on internal template motifs after realignment of the 3' termini. *Proc Natl Acad Sci U S A* **108,** 7206-7211 (2011).
18. Garcin, D., Lezzi, M., Dobbs, M., Elliott, R. M., *et al.* The 5' ends of Hantaan virus (Bunyaviridae) RNAs suggest a prime-and-realign mechanism for the initiation of RNA synthesis. *J Virol* **69,** 5754-5762 (1995).
19. Koppstein, D., Ashour, J. & Bartel, D. P. Sequencing the cap-snatching repertoire of H1N1 influenza provides insight into the mechanism of viral transcription initiation. *Nucleic Acids Res* **43,** 5052-5064 (2015).
20. Chung, T. D., Cianci, C., Hagen, M., Terry, B., *et al.* Biochemical studies on capped RNA primers identify a class of oligonucleotide inhibitors of the

influenza virus RNA polymerase. *Proc Natl Acad Sci U S A* **91,** 2372-2376 (1994).
21. Lukarska, M., Fournier, G., Pflug, A., Resa-Infante, P., *et al.* Structural basis of an essential interaction between influenza polymerase and Pol II CTD. *Nature* **541,** 117-121 (2016).
22. Martínez-Alonso, M., Hengrung, N. & Fodor, E. RNA-Free and Ribonucleoprotein-Associated Influenza Virus Polymerases Directly Bind the Serine-5-Phosphorylated Carboxyl-Terminal Domain of Host RNA Polymerase II. *J Virol* **90,** 6014-6021 (2016).
23. Plotch, S. J., Bouloy, M., Ulmanen, I. & Krug, R. M. A unique cap(m7GpppXm)-dependent influenza virion endonuclease cleaves capped RNAs to generate the primers that initiate viral RNA transcription. *Cell* **23,** 847-858 (1981).
24. Sikora, D., Rocheleau, L., Brown, E. G. & Pelchat, M. Deep sequencing reveals the eight facets of the influenza A/HongKong/1/1968 (H3N2) virus cap-snatching process. *Sci Rep* **4,** 6181 (2014).
25. Geerts-Dimitriadou, C., Goldbach, R. & Kormelink, R. Preferential use of RNA leader sequences during influenza A transcription initiation in vivo. *Virology* **409,** 27-32 (2011).
26. Poon, L. L., Pritlove, D. C., Fodor, E. & Brownlee, G. G. Direct evidence that the poly (A) tail of influenza A virus mRNA is synthesized by reiterative copying of a U track in the virion RNA template. *Journal of virology* **73,** 3473-3476 (1999).
27. Krug, R. M., Broni, B. A., LaFiandra, A. J., Morgan, M. A. & Shatkin, A. J. Priming and inhibitory activities of RNAs for the influenza viral transcriptase do not require base pairing with the virion template RNA. *Proceedings of the National Academy of Sciences* **77,** 5874-5878 (1980).
28. Geerts-Dimitriadou, C., Zwart, M. P., Goldbach, R. & Kormelink, R. Base-pairing promotes leader selection to prime in vitro influenza genome transcription. *Virology* **409,** 17-26 (2011).
29. Vreede, F. T. & Brownlee, G. G. Influenza virion-derived viral ribonucleoproteins synthesize both mRNA and cRNA in vitro. *J Virol* **81,** 2196-2204 (2007).

30. Jung, T. E. & Brownlee, G. G. A new promoter-binding site in the PB1 subunit of the influenza A virus polymerase. *J Gen Virol* **87,** 679-688 (2006).
31. Du, Y., Wu, N. C., Jiang, L., Zhang, T., *et al.* Annotating Protein Functional Residues by Coupling High-Throughput Fitness Profile and Homologous-Structure Analysis. *MBio* **7,** (2016).
32. Laurila, M. R., Makeyev, E. V. & Bamford, D. H. Bacteriophage phi 6 RNA-dependent RNA polymerase: molecular details of initiating nucleic acid synthesis without primer. *J Biol Chem* **277,** 17117-17124 (2002).
33. Hong, Z., Cameron, C. E., Walker, M. P., Castro, C., *et al.* A novel mechanism to ensure terminal initiation by hepatitis C virus NS5B polymerase. *Virology* **285,** 6-11 (2001).
34. Mosley, R. T., Edwards, T. E., Murakami, E., Lam, A. M., *et al.* Structure of hepatitis C virus polymerase in complex with primer-template RNA. *J Virol* **86,** 6503-6511 (2012).
35. Appleby, T. C., Perry, J. K., Murakami, E., Barauskas, O., *et al.* Structural basis for RNA replication by the hepatitis C virus polymerase. *Science* **347,** 771-775 (2015).
36. Tomescu, A. I., Robb, N. C., Hengrung, N., Fodor, E. & Kapanidis, A. N. Single-molecule FRET reveals a corkscrew RNA structure for the polymerase-bound influenza virus promoter. *Proc Natl Acad Sci USA* **111,** E3335-E3342 (2014).
37. Fodor, E., Crow, M., Mingay, L. J., Deng, T., *et al.* A single amino acid mutation in the PA subunit of the influenza virus RNA polymerase inhibits endonucleolytic cleavage of capped RNAs. *J Virol* **76,** 8989-9001 (2002).
38. Deng, T., Sharps, J., Fodor, E. & Brownlee, G. G. In vitro assembly of PB2 with a PB1-PA dimer supports a new model of assembly of influenza A virus polymerase subunits into a functional trimeric complex. *J Virol* **79,** 8669-8674 (2005).
39. Kerry, P. S., Willsher, N. & Fodor, E. A cluster of conserved basic amino acids near the C-terminus of the PB1 subunit of the influenza virus RNA polymerase is involved in the regulation of viral transcription. *Virology* **373,** 202-210 (2008).
40. Lee, M. T., Bishop, K., Medcalf, L., Elton, D., *et al.* Definition of the minimal viral components required for the initiation of unprimed RNA

synthesis by influenza virus RNA polymerase. *Nucleic Acids Res* **30,** 429-438 (2002).
41. te Velthuis, A. J. Common and unique features of viral RNA-dependent polymerases. *Cell Mol Life Sci* **71,** 4403-4420 (2014).
42. Lee, M. -K., Bae, S. -H., Park, C. -J., Cheong, H. -K., *et al.* A single-nucleotide natural variation (U4 to C4) in an influenza A virus promoter exhibits a large structural change: implications for differential viral RNA synthesis by RNA-dependent RNA polymerase. *Nucleic acids research* **31,** 1216-1223 (2003).
43. Hagen, M., Tiley, L., Chung, T. D. & Krystal, M. The role of template-primer interactions in cleavage and initiation by the influenza virus polymerase. *J Gen Virol* **76 (Pt 3),** 603-611 (1995).
44. Datta, K., Wolkerstorfer, A., Szolar, O. H., Cusack, S. & Klumpp, K. Characterization of PA-N terminal domain of Influenza A polymerase reveals sequence specific RNA cleavage. *Nucleic Acids Res* **41,** 8289-8299 (2013).
45. Tao, Y., Farsetta, D. L., Nibert, M. L. & Harrison, S. C. RNA synthesis in a cage—structural studies of reovirus polymerase lambda3. *Cell* **111,** 733-745 (2002).
46. Nilsson, B. E., Te Velthuis, A. J. & Fodor, E. Role of the PB2 627 Domain in Influenza A Virus Polymerase Function. *J Virol* **91,** (2017).
47. van Knippenberg, I., Lamine, M., Goldbach, R. & Kormelink, R. Tomato spotted wilt virus transcriptase in vitro displays a preference for cap donors with multiple base complementarity to the viral template. *Virology* **335,** 122-130 (2005).
48. Bouloy, M., Pardigon, N., Vialat, P., Gerbaud, S. & Girard, M. Characterization of the 5' and 3' ends of viral messenger RNAs isolated from BHK21 cells infected with Germiston virus (Bunyavirus). *Virology* **175,** 50-58 (1990).
49. Duijsings, D., Kormelink, R. & Goldbach, R. In vivo analysis of the TSWV cap-snatching mechanism: single base complementarity and primer length requirements. *EMBO J* **20,** 2545-2552 (2001).
50. Vreede, F. T., Jung, T. E. & Brownlee, G. G. Model suggesting that replication of influenza virus is regulated by stabilization of replicative intermediates. *J Virol* **78,** 9568-9572 (2004).

51. Hara, K., Schmidt, F. I., Crow, M. & Brownlee, G. G. Amino acid residues in the N-terminal region of the PA subunit of influenza A virus RNA polymerase play a critical role in protein stability, endonuclease activity, cap binding, and virion RNA promoter binding. *J Virol* **80,** 7789-7798 (2006).
52. Larkin, M. A., Blackshields, G., Brown, N. P., Chenna, R., *et al.* Clustal W and Clustal X version 2.0. *Bioinformatics* **23,** 2947-2948 (2007).
53. Robert, X. & Gouet, P. Deciphering key features in protein structures with the new ENDscript server. *Nucleic Acids Res* **42,** W320-W324 (2014).
54. York, A., Hutchinson, E. C. & Fodor, E. Interactome analysis of the influenza A virus transcription/replication machinery identifies protein phosphatase 6 as a cellular factor required for efficient virus replication. *J Virol* **88,** 13284-13299 (2014).
55. Kapanidis, A. N., Lee, N. K., Laurence, T. A., Doose, S., *et al.* Fluorescence-aided molecule sorting: analysis of structure and interactions by alternating-laser excitation of single molecules. *Proc Natl Acad Sci U S A* **101,** 8936-8941 (2004).
56. Santoso, Y., Hwang, L. C., Le Reste, L. & Kapanidis, A. N. Red light, green light: probing single molecules using alternating-laser excitation. *Biochem Soc Trans* **36,** 738-744 (2008).

Figures

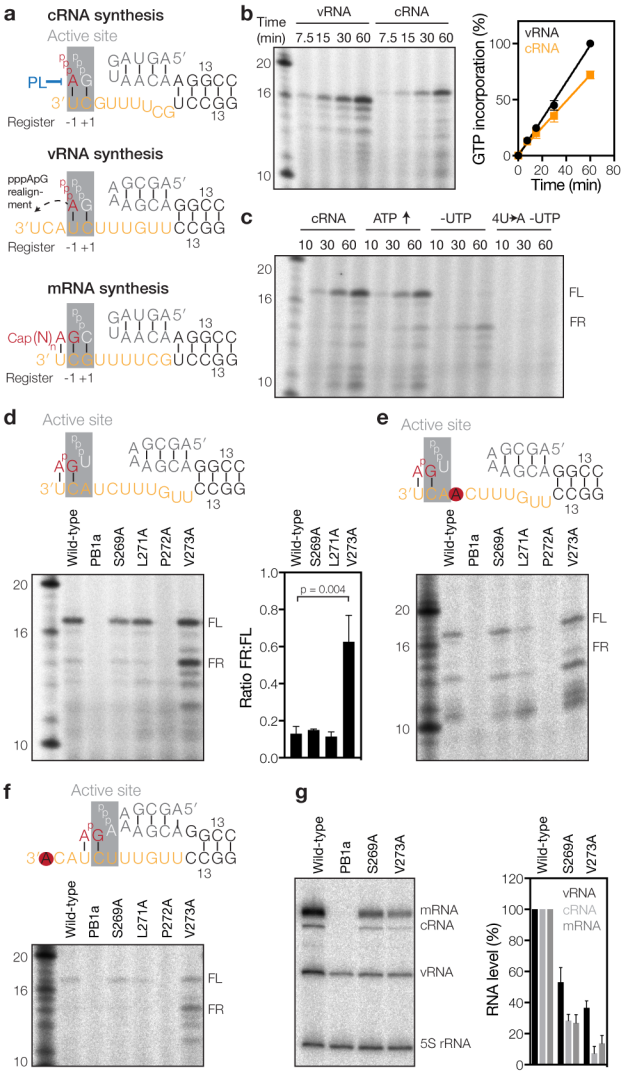

Figure 1. Realignment is essential for viral RNA synthesis. (**a**) Models of IAV initiation during cRNA, vRNA and mRNA synthesis. The priming loop (PL) is indicated in blue. The active site (grey) positions -1 and +1 are indicated below each schematic. (**b**) Time course of ApG extension on a vRNA or cRNA promoter. The graph shows the percentage of [α-^{32}P]GTP incorporation normalised to the activity on the vRNA promoter. Error bars indicate standard deviation (*n* = 3). (**c**) Time course of ApG extension on a wild-type or 4U→A mutant cRNA promoter. Additions of 0.5 mM ATP and the omission of UTP are indicated. (**d**) ApG extension on a cRNA promoter. The graph shows the mean failed realignment product to full-length product ratio of three independently purified sets of RdRps. The p-value was determined using an unpaired non-parametric t-test. (**e**) ApG extension on the mutant cRNA promoter 4U→A. (**f**) ApG extension on the mutant cRNA promoter 1U→A. (**g**) Analysis of the steady state NA RNA

levels in RNP reconstitution assays. The graph shows the mean RNA levels of three independent experiments. In each graph the error bars indicate standard deviation (n = 3). For all activity assays, we used three independently purified IAV RdRp sets isolated from 293T cells.

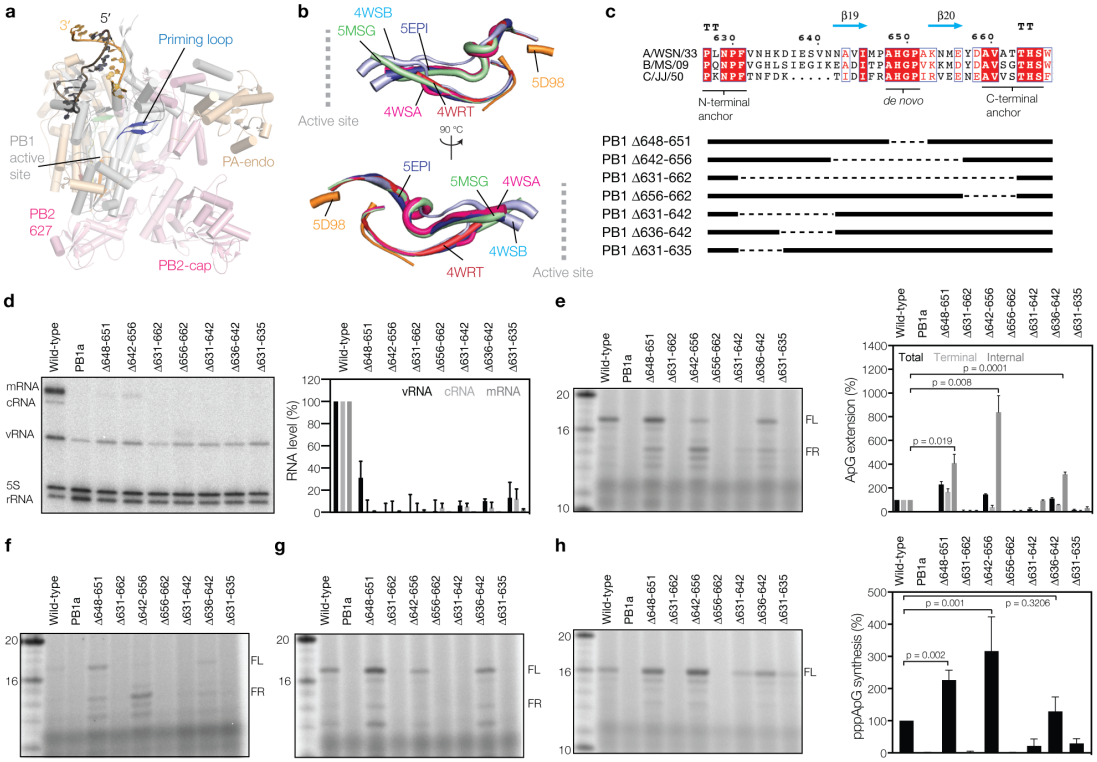

Figure 2. Deletions in the priming loop affect realignment and viral RNA synthesis in cell culture. (**a**) Position of the priming loop relative to the active site and promoter binding pocket of the IAV RdRp (PDB 4WSB). For clarity, only the right side of the RdRp is shown. (**b**) Superposed structures of the bat IAV priming loop (PDB 4WSB), influenza B virus priming loop (PDBs 5MSG, 4WSA, 4WRT and 5EPI) and the influenza C virus priming loop (PDB 5D98). The thickness of the backbone is scaled by β-factor to illustrate the flexible parts of the priming loop. (**c**) Alignment of the PB1 amino acid sequences that constitute the priming loop of the IAV A/WSN/33 (H1N1), influenza B virus B/Michigan/22687/09, and influenza C virus C/JJ/50 RdRps. Identical residues are shaded red and conserved residues are surrounded with blue boxes. Secondary structure annotations are based on PDB 4WSB. Deletions in the priming loop are indicated with dotted lines. (**d**) Analysis of the steady state viral NA RNA levels. The graph shows the mean RNA levels with error bars indicating standard deviation (*n* = 3). (**e**) ApG extension on a cRNA promoter. Graph shows mean activity and error bars indicate standard deviation (*n* = 3). (**f**) ApG extension on the mutant cRNA promoter 1U→A (**g**) ApG extension

on the mutant cRNA promoter 4U→A. (**h**) ApG extension on a wild-type vRNA promoter. Graph shows mean activity with error bars indicating standard deviation (*n* = 3). In panel e and h, p-values were determined using an unpaired non-parametric t-test. For all activity assays, we used three independently purified IAV RdRp sets isolated from 293T cells.

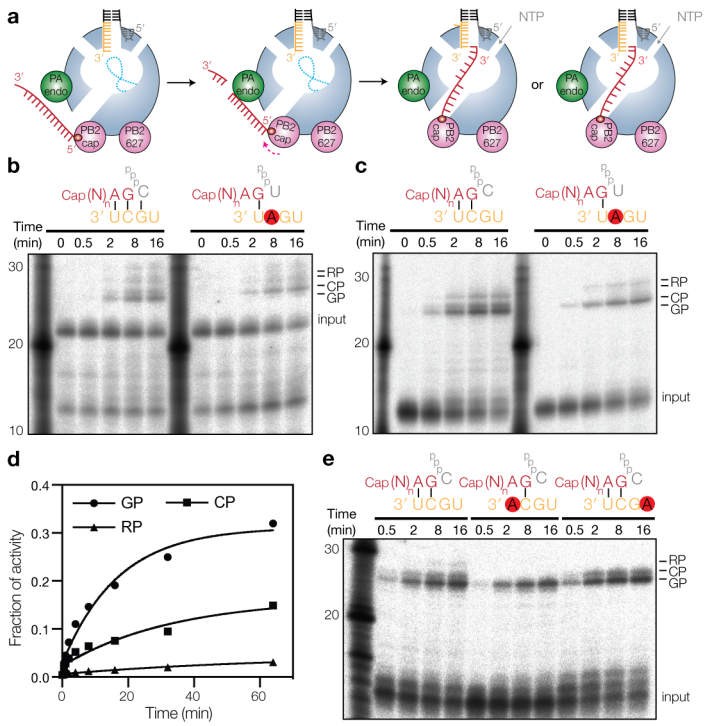

Figure 3. Realignment during transcription initiation. (**a**) Schematic of cap cleavage and transcription initiation with a capped 11 nucleotide long primer. The initiation from positions 2C or 3G is depicted. (**b**) Cleavage and extension of a capped 20-nucleotide long RNA in the presence of four NTPs. The products produced from position 2C (CP) and 3G (GP) as well as the realignment product (RP) are indicated. The schematic shows the expected initiation site on the wild-type or mutant 3' promoter strand. (**c**) Extension of a radiolabelled capped 11-nucleotide long RNA in the presence of four NTPs. (**d**) Accumulation of the GP, CP and RP signals as fraction of the total transcriptional activity. Lines represent fits to an exponential decay of one representative experiment (Supplemental Fig. 4b). (**e**) Extension of a radiolabelled capped 11-nucleotide long RNA in the presence of unlabelled NTPs. In all activity assays, we used IAV RdRp preparations purified from insect cells.

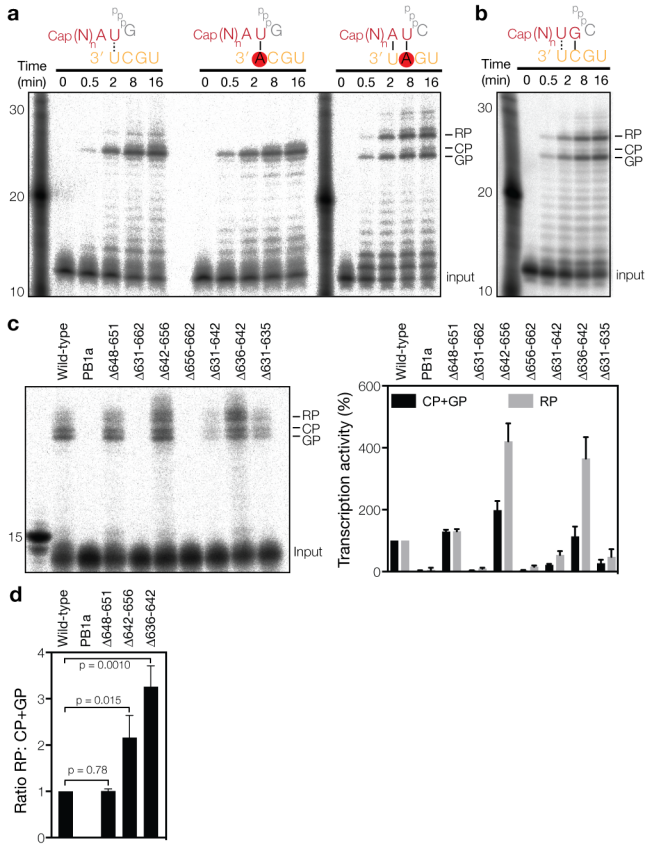

Figure 4. The priming loop modulates transcription initiation. (**a** and **b**) Extension of a radiolabelled capped 11-nucleotide long RNA in the presence of unlabelled NTPs and IAV RdRp purified from insect cells. The schematic shows the expected initiation site on the wild-type or mutant 3' promoter strand. (**c**) Extension of a radiolabelled capped 11-nucleotide ending in 3' AG in the presence of wild-type or mutant IAV RdRp purified from 293T cells. The graph shows the mean accumulation of transcription products initiated from 3G and 2C (GP+CP) or produced after realignment (RP). Error bars show standard deviations (*n* = 3). (**d**) Efficiency of realignment normalised to the transcription initiation activity. Error bars show standard deviations (*n* = 3). The p-values were determined using an unpaired non-parametric t-test.

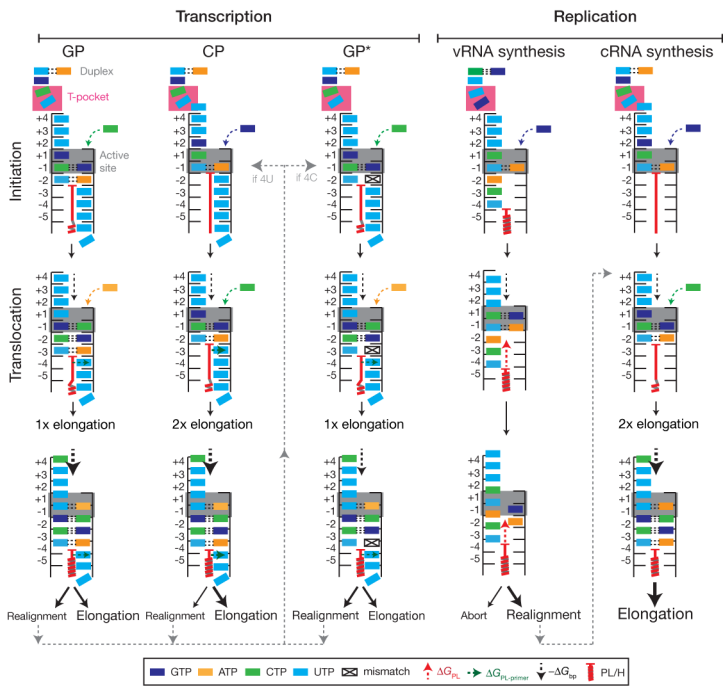

Figure 5. Model of influenza A virus RNA synthesis. IAV **transcription** can initiate with a capped primer that fully base pairs with the 3' 1U and 2C of the vRNA (GP formation), or a primer that base pairs only with the 3' 1U (CP formation) or one that is only base paired via 2C and mismatched at 3' 1U (GP* formation). The priming loop stabilises the capped primer in the active site ($\Delta G_{PL\text{-}primer}$). When the 3' 1U of the vRNA leaves position -4 of the active site, realignment may occur depending of the stability of the template-primer duplex. On a vRNA promoter containing a 3' 4U, realignment will proceed (grey dotted line) via the CP pathway. On a vRNA promoter contain a 3' 4C (segment 1, 2, and 3 of the IAV genome), realignment will proceed via the GP* pathway. It is known that this mutation down regulates transcription[42]. **vRNA synthesis** during IAV replication is catalysed from cRNA residues 3' 4U and 5C when these occupy position -1 and +1 of the active site. The 3' 1U of the cRNA then occupies position -4. After dinucleotide formation, the priming loop blocks (ΔG_{PL}) translocation of 3' 1U to position -5, which results in melting of the template-dinucleotide duplex. The cRNA 3' terminus can now ratchet back 2 positions until 3' 1U occupies position -2 to facilitate hybridisation with the dinucleotide. vRNA extension now becomes effectively similar to cRNA synthesis (grey dotted line). **cRNA synthesis** is initiated on 3' 1U and 2C of the vRNA when these occupy position -1 and +1 of the active

site. To stabilise the initiating ATP, an interaction with the tip of the priming loop is required. Translocation is not hindered by the priming loop after initiation, allowing two elongation steps until a tetramer is formed. Then the stability of the template-product duplex ($-\Delta G_{bp}$) is likely high enough to induce a conformational change, potentially similar to HCV elongation[35], to facilitate progressive elongation. The priming loop/palm subdomain influences are drawn as a single red coiled structure for simplicity. The probability of realignment or elongation is indicated by the font size.